TENDENCIES TO THE DEVELOPMENT AND PROBLEMS OF LASER SOUNDING OF ATMOSPHERIC POLLUTIONS

V.M. Dubyagin and N.A. Shefer

Institute of Atmospheric Optics,
Siberian Branch of the Russian Academy of Sciences, Tomsk
Received October 21, 1992

Tendencies to the development of ecological lidars are outlined. The necessity is justified to develop mobile gas and aerosol UV–lidars for sounding of the pollution sources. Certain problems arising in the development of such lidars are discussed. A unique technique for solving the transmission problems as well as some aspects of this problem in the case of using the fourth harmonic of a Nd : YAG laser are discussed.

INTRODUCTION

Ecological monitoring of atmospheric pollutions becomes more urgent problem with extending industrial activity.[1] Lidar can be one of the effective systems operating in a network of ecological stations.

Dust, aerosol, and gases are known to be the main atmospheric pollutants. Most of their mass is distributed over the atmospheric ground layer and, moreover, not far from pollution sources.[2] Therefore, sounding of sources of gaseous and aerosol emissions such as plant stacks, pits, highways, etc. is the most important primary stage of the air pollution monitoring.

TENDENCIES TO THE DEVELOPMENT OF ECOLOGICAL LIDARS

The lidars are the optical devices which are permanently improved to satisfy concrete applications better, including the ecological one.[3,4] There appeared a class of elastic–scattering (ES) lidars capable of sounding the dust and aerosol components (fractions).[5] Usually, these lidars were produced in a stationary version[6] with an operation range of a few kilometres. Two directions based on using the phenomena of resonance absorption and Raman scattering (RS) were simultaneously developed for sounding of gas pollutants.[7,8] A successful development of the first has led to creating a class of the gas analyzers[9] for measuring the concentration of a sounded gas averaged over the path from a laser to retroreflector and a class of differential absorption lidars (DIAL)[10] possessing a spatial resolution. The differential absorption lidars, as a rule, were intended for sounding of a single gas pollutant at a distance of hundreds of meters or several kilometres. Of course, such lidars equipped with tunable lasers can monitor several pollutants, but the cost of such an equipment is very high.[11]

The RS phenomenon was first used for creating spontaneous Raman scattering (SRS) lidars. The lidars were proved to be effective for sounding at a distance of several tens and hundreds of meters, but only of very dusted areas.[12] However, they were capable of monitoring several pollutants simultaneously. Work is now underway toward the construction of resonance Raman scattering (RRS) lidars[13] which are expected to have longer distance of operation, but allow one to monitor, as a rule, only one gas component. One more class of lidars intended for sounding of gas pollutants and based on using a resonance fluorescence phenomenon has found only limited application because of its low efficiency.[14]

All the above–mentioned lidars have certain disadvantages which give no way for monitoring of numerous widely spread sources of atmospheric emissions in real time. Therefore, there exists the necessity of creating a new class of mobile and inexpensive lidars capable of sounding industrial aerosol and gas pollutants simultaneously from a distance of several hundreds of meters in any direction at any time of day and night.

An integrated gas and aerosol lidar can be most easily performed by combining in one instrument the functions of the ES and SRS lidars. Consequently, it is sufficient to have any laser with arbitrary wavelength in transmitting system and a spectral device similar to a triple monochromator with a collection of filters, attenuators, and detectors, allowing one to record the RS– and ES–signals in the photon counting regime, in receiving system.[12] At present it is not a problem[15] to mount such a lidar equipped with a scanning system on a chassis. For the lidar to be able to operate at any time one should use a laser emitting within the wavelength interval from 250 to 280 nm.[8] At present a solid–state Nd : YAG laser with radiation conversion into the fourth harmonic (266 nm) is widely used due to its reliability, simplicity, and low cost,[3,4,7] though the use of excimer and dye lasers is possible.[8]

For providing a high efficiency of the proposed integrated ecological lidar it is necessary to solve a number of problems.

PROBLEMS OF INTEGRATED ECOLOGICAL SOUNDING

Usually, atmospheric nitrogen[3] is used as a reference gas when determining the number density of the gas being sounded. In so doing the concentration of nitrogen is assumed to be known and equal to the background one. However, at the exit from atmospheric emission sources we have, as a rule, a high–temperature aggressive medium.[1] For these media the nitrogen concentration should be determined taking into account the pressure and temperature of the medium, measured directly during sounding, and chemical reactions of the type $N_2O + O \rightarrow N_2 + O_2 \rightarrow 2NO$.

Use of a UV laser provides narrowing of the wavelength range of SRS in the medium, shifting it closer to the sounding wavelength and to the threshold of

0235-6880/92/10 717-08 $02.00

spectral sensitivity of known types of PMT's.[17] All these impose certain requirements on the characteristics of employed spectral devices and PMT's. These requirements can be met with a triple monochromator[18] which has a coefficient of suppression of ~ 10^{12} at unshifted wavelength, transparency of ~ 4% at wavelengths of the SRS, linear dispersion 0.25–0.75 nm/mm, filtered–out bandwidth of ~ 20 cm^{-1}, and PMT FÉU–106 (see Ref. 17) having a quantum efficiency of ~ 0.3 in the region > 160 nm, magnification coefficient of ~ 10^7, and dark–count rate 20–100 Hz.

Quantitative measurements of concentration of pollutants require a knowledge of RS cross sections of the corresponding gases. Though the relative RS cross sections have been measured for many gases,[4] their use in the case of UV–exciting radiation should be very careful. The matter is that a number of gases, for example, O_2, O_3, NO_2, SO_2, C_6H_6, HNO_3, H_2O_2, N_2O_5, and others have lines and bands of absorption in the UV and for them the resonance Raman scattering (RRS) can be observed with the cross sections being by several orders of magnitude greater than the SRS cross section.[7] Thus, the resonance increase of the cross section due to exciting radiation at 266 nm is equal to 1.95 for O_2 and 150 for C_6H_6. At present there exist only a few semiempirical methods (see a review in Ref. 7) allowing one to estimate the values of the RS cross section of any gases for an arbitrary exciting wavelengths. Because of a complexity, low precision, and poor reliability these methods require additional measurements of the RS cross sections of gases in the UV. Moreover, for high–temperature media being sounded a correction for different population of the ground level at different temperatures[14] must be introduced in the cross sections.

Relations for determining the concentrations of the gases being sounded involve[12] the ratios of atmospheric transmissions at the SRS wavelengths of the gases to that at the wavelength of the nitrogen SRS line, as well as to the transmission at the wavelength of sounding radiation. These ratios, of course, should be known very accurately. For the case of the UV sounding of the atmospheric emission sources this problem is very important because of several reasons. First, strong electronic absorption bands of many gases are in the range 250–300 nm.[19] Second, concentrations of these gases and aerosol near the source are so high[1,2,20] that even at a distance of tens of meters the values of transmission essentially differ from unity. Third, a substance of plumes is not "grey" for the UV, i.e., a strong spectral dependence of absorption takes place.[14] Fourth, concentrations of the gases and aerosol in plumes have a very complicated spatiotemporal distribution because of nonstationarity of the sources and perturbation effect of the atmosphere.[1] Up to now the ratios of transmissions either were roughly assumed to be equal to unity or were *a priori* estimated using model coefficients of aerosol extinction and Rayleigh scattering and model profiles of absorbing gas concentrations.[8] It is obvious that such a solution of the problem in the considered case gives low accuracy of the final results of measurements. Therefore, we have developed[21] a special technique of an account of transmissions with the help of which effective algorithms for signal processing in integrated ecological sounding can be obtained.

METHOD OF AN *A POSTERIORI* ACCOUNT OF THE TRANSMISSIONS

The method is based on the possibility of retrieving almost all necessary *a priori* information directly from lidar data obtained with a specially designed receiver for special geometry of sounding. The receiver should have the following recording channels: aerosol, nitrogen, gases being sounded, and possibly, some of the absorbing gases. The lidar should be located on the windward side of the emission source, at a distance at which the first gates are yet in the relatively clear atmosphere.

Concentrations of sounded $M_1, \ldots, M_i, \ldots, M_I$ and absorbing $L_1, \ldots, L_j, \ldots, L_J$ gases, air M_{air}, and aerosol M_{a} in the kth strobe are found by any iteration method by simultaneous solution of the following system of nonlinear equations:

$$M_1^{(k)} \sim F_1\left(M_{\text{air}}^{(1)}, \ldots, M_{\text{air}}^{(k)}; M_{\text{a}}^{(1)}, \ldots, M_{\text{a}}^{(k)}; \mathbf{L}^{(1)}, \ldots, \mathbf{L}^{(k)}\right);$$

$$\vdots$$

$$M_I^{(k)} \sim F_I\left(M_{\text{air}}^{(1)}, \ldots, M_{\text{air}}^{(k)}; M_{\text{a}}^{(1)}, \ldots, M_{\text{a}}^{(k)}; \mathbf{L}^{(1)}, \ldots, \mathbf{L}^{(k)}\right);$$

$$L_1^{(k)} \sim \varphi_1\left(M_{\text{air}}^{(1)}, \ldots, M_{\text{air}}^{(k)}; M_{\text{a}}^{(1)}, \ldots, M_{\text{a}}^{(k)}; \mathbf{L}^{(1)}, \ldots, \mathbf{L}^{(k)}\right);$$

$$\vdots$$

$$L_J^{(k)} \sim \varphi_J\left(M_{\text{air}}^{(1)}, \ldots, M_{\text{air}}^{(k)}; M_{\text{a}}^{(1)}, \ldots, M_{\text{a}}^{(k)}; \mathbf{L}^{(1)}, \ldots, \mathbf{L}^{(k)}\right);$$

$$M_{\text{air}}^{(k)} \sim \psi\left(M_{\text{air}}^{(1)}, \ldots, M_{\text{air}}^{(k)}; M_{\text{a}}^{(1)}, \ldots, M_{\text{a}}^{(k)}; \mathbf{L}^{(1)}, \ldots, \mathbf{L}^{(k)}\right);$$

$$M_{\text{a}}^{(k)} \sim f\left(M_{\text{air}}^{(1)}, \ldots, M_{\text{air}}^{(k)}; M_{\text{a}}^{(1)}, \ldots, M_{\text{a}}^{(k)}; \mathbf{L}^{(1)}, \ldots, \mathbf{L}^{(k)}\right).$$

Here, $F_1, \ldots, F_i, \ldots, F_I$, $\varphi_1, \ldots, \varphi_j, \ldots, \varphi_J$, f, and ψ describe the functional dependences of the corresponding ratios of transmissions to the transmission at the wavelength of the SRS line of nitrogen on the concentrations of air, aerosol, and absorption gases in the first k strobes.

The value of concentration obtained by extrapolation of the concentrations already estimated in the preceding strobes is taken as the initial approach in the kth strobe. In the first strobe the background concentration is taken as the initial approach. The number of absorbing gases is different depending on the type of the emission source, but usually it is no more than ten. Therefore, the use of this number of the RS channels is not difficult. Moreover, absorbing gases frequently are the gases to be sounded that essentially simplifies the processing algorithm.

SOME ASPECTS OF THE TRANSMISSION PROBLEM WHEN SOUNDING AT 266 nm

If the fourth harmonic of a Nd : YAG laser is used for RS excitation, the wavelengths of the RS of all atmospheric gases are within the interval from 270 to 300 nm. In this interval the following gases (see Table I) have absorption spectra arranged according to the decreasing absorption cross sections: O_3 (Ref. 22), SO_2

(Refs. 23, 24), HO_2NO_2 (Ref. 25), NO_5 (Ref. 26), NO_2 (Ref. 25), H_2O_2 (Ref. 26), HNO_3 (Ref. 27), C_3H_6O (Ref. 28), Cl_2 (Ref. 29), HNO_2 (Ref. 30), $C_2H_2O_2$, and C_2H_4O (Ref. 28), ClO, ClO_3, ClOO, ClONO, $ClNO_2$, $BrONO_2$, ClNO, $ClONO_2$, HOCl, CF_2Br_2, $COCl_2$, CH_3Br, and $HClO_4$ (Ref. 31).

The decisive role in the transmission problem belongs not to the absolute values of the cross sections but to their differences at the corresponding wavelengths and, more exactly, the differences between the absorption coefficients. In this sense O_3, SO_2, NO_2, and HNO_3 are most important. This is illustrated by Fig. 1 which shows the concentrations of these gases resulting in a 1% systematic error in the estimate of the concentrations of gases being sounded along 1–km path. It is shown that absorption by the following gases should be taken into account: ozone when sounding practically all gases even in the background atmosphere, sulphur dioxide when sounding many gases in the background and all gases in dusty atmosphere, nitrogen peroxide when sounding gases in the polluted atmosphere, and nitrogen acid when sounding the pollution sources. Calculation of absorption by other gases may be needed only when sounding the pollution sources.

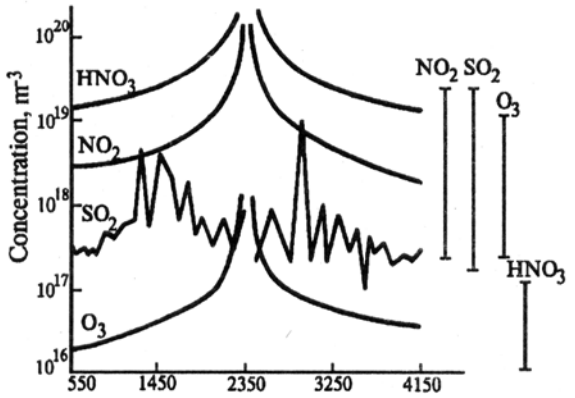

FIG. 1. The maximum admissible concentrations of absorbing gases O_3, SO_2, NO_2, *and* HNO_3 *as functions of the Raman shift. Vertical lines show the range of concentration variations of gases in the atmosphere from the background under rural conditions to that under polluted urban conditions.*

The sounding distance is one of the key parameters for the transmission problem. It is obvious that in some cases a mobile lidar can be installed very close to a sounded volume in order to bring the ratio of transmissions close to unity. However, as can be seen from Fig. 2, these cases reduced only to sounding of the background or dusty atmosphere rather than to sounding of the pollution sources. Thus, the effect of SO_2 is well–pronounced at a distance of hundreds of meters in the urban several atmosphere, several meters in plumes, and several centimeters at the stack input.

TABLE I. Gas absorption cross sections, m^2.

Wavelength, nm	SO_2	O_3	NO_2	HNO_3	H_2O_2
269.9	3.70E–23	7.90E–22	3.12E–24	1.63E–24	3.56E–24
270.0	3.60E–23	7.91E–22	3.13E–24	1.63E–24	3.55E–24
270.3	2.80E–23	7.78E–22	3.18E–24	1.62E–24	3.50E–24
270.9	3.50E–23	7.53E–22	3.29E–24	1.59E–24	3.41E–24
271.3	3.00E–23	7.38E–22	3.35E–24	1.57E–24	3.35E–24
271.6	3.48E–23	7.24E–22	3.41E–24	1.56E–24	3.29E–24
271.8	3.10E–23	7.16E–22	3.45E–24	1.55E–24	3.26E–24
272.6	4.70E–23	6.82E–22	3.59E–24	1.51E–24	3.13E–24
273.1	4.40E–23	6.62E–22	3.68E–24	1.49E–24	3.05E–24
274.1	8.30E–23	6.22E–22	3.86E–24	1.44E–24	2.89E–24
274.7	5.30E–23	5.98E–22	3.97E–24	1.41E–24	2.80E–24
275.2	6.50E–23	5.78E–22	4.08E–24	1.39E–24	2.72E–24
275.9	4.60E–23	5.53E–22	4.28E–24	1.36E–24	2.64E–24
276.7	6.90E–23	5.24E–22	4.52E–24	1.31E–24	2.53E–24
277.7	6.20E–23	4.85E–22	4.84E–24	1.26E–24	2.39E–24
278.3	8.20E–23	4.64E–22	5.02E–24	1.23E–24	2.31E–24
278.9	6.25E–23	4.46E–22	5.19E–24	1.20E–24	2.24E–24
279.5	8.90E–23	4.34E–22	5.39E–24	1.17E–24	2.16E–24
280.0	5.40E–23	4.19E–22	5.54E–24	1.14E–24	2.09E–24
281.0	9.80E–23	3.83E–22	5.83E–24	1.09E–24	2.00E–24
281.8	5.40E–23	3.51E–22	6.06E–24	1.05E–24	1.94E–24
282.6	9.90E–23	3.21E–22	6.29E–24	1.00E–24	1.87E–24
283.4	5.70E–23	2.95E–22	6.53E–24	9.61E–25	1.80E–24
283.6	6.70E–23	2.88E–22	6.58E–24	9.51E–25	1.78E–24
284.6	1.12E–22	2.59E–22	6.87E–24	8.98E–25	1.69E–24
285.8	5.70E–23	2.28E–22	7.18E–24	8.38E–25	1.59E–24
287.5	1.12E–22	1.90E–22	7.59E–24	7.56E–25	1.45E–24
288.3	6.80E–23	1.76E–22	7.76E–24	7.19E–25	1.38E–24
289.2	1.08E–22	1.59E–22	7.99E–24	6.73E–25	1.30E–24
290.2	7.60E–23	1.43E–22	8.22E–24	6.28E–25	1.22E–24
290.6	1.09E–22	1.35E–22	8.36E–24	6.09E–25	1.20E–24
291.6	5.60E–23	1.18E–22	8.66E–24	5.67E–25	1.15E–24
292.5	1.00E–22	1.05E–22	8.93E–24	5.3 E–25	1.10E–24
293.3	4.90E–23	9.57E–23	9.15E–24	4.99E–25	1.06E–24
294.0	1.50E–22	8.70E–23	9.37E–24	4.68E–25	1.02E–24
294.2	8.80E–23	8.48E–23	9.43E–24	4.59E–25	1.01E–24
294.6	1.01E–22	8.06E–23	9.55E–24	4.43E–25	.990E–24
295.5	4.20E–23	7.19E–23	9.87E–24	4.11E–25	9.43E–25
296.4	1.12E–22	6.42E–23	1.02E–23	3.84E–25	8.96E–25
297.4	3.20E–23	5.67E–23	1.06E–23	3.54E–25	8.44E–25
298.2	1.08E–22	5.13E–23	1.10E–23	3.3E–25	8.02E–25
299.1	3.90E–23	4.62E–23	1.13E–23	3.04E–25	7.57E–25
269.9	1.52E–23	2.87E–23	2.20E–25	3.79E–25	9.51E–26
270.0	1.52E–23	2.80E–23	2.20E–25	3.80E–25	9.81E–26
270.3	1.51E–23	2.77E–23	2.24E–25	4.05E–25	1.16E–25
270.9	1.48E–23	2.71E–23	2.32E–25	4.54E–25	1.51E–25
271.3	1.46E–23	2.68E–23	2.37E–25	4.83E–25	1.74E–25
271.6	1.45E–23	2.64E–23	2.42E–25	5.11E–25	1.98E–25
271.8	1.44E–23	2.62E–23	2.44E–25	5.28E–25	2.12E–25
272.6	1.40E–23	2.54E–23	2.55E–25	5.93E–25	2.79E–25

TABLE I. (continued).

Wavelength, nm	N_2O_5	HO_2NO_2	HNO_2	Cl_2	$C_2H_2O_2$
273.1	1.38E–23	2.49E–23	2.62E–25	6.34E–25	3.22E–25
274.1	1.34E–23	2.39E–23	2.75E–25	7.16E–25	4.02E–25
274.7	1.31E–23	2.33E–23	2.83E–25	7.65E–25	4.61E–25
275.2	1.29E–23	2.28E–23	2.90E–25	8.06E–25	5.10E–25
275.9	1.26E–23	2.22E–23	2.99E–25	8.60E–25	5.74E–25
276.7	1.22E–23	2.14E–23	3.10E–25	9.25E–25	6.40E–25
277.7	1.17E–23	2.03E–23	3.24E–25	1.01E–24	7.50E–25
278.3	1.15E–23	1.97E–23	3.32E–25	1.06E–24	8.14E–25
278.9	1.12E–23	1.92E–23	3.39E–25	1.11E–24	8.68E–25
279.5	1.09E–23	1.85E–23	3.48E–25.	1.16E–24	9.32E–25
280.0	1.07E–23	1.80E–23	3.55E–25	1.2 E–24	9.81E–25
281.0	1.02E–23	1.72E–23	3.71E–25	1.36E–24	1.12E–24
281.8	9.84E–24	1.66E–23	3.84E–25	1.49E–24	1.24E–24
282.6	9.45E–24	1.59E–23	3.97E–25	1.62E–24	1.37E–24
283.4	9.07E–24	1.53E–23	4.09E–25	1.74E–24	1.51E–24
283.6	8.97E–24	1.51E–23	4.13E–25	1.78E–24	1.55E–24
284.6	8.49E–24	1.43E–23	4.29E–25	1.94E–24	1.76E–24
285.8	7.98E–24	1.35E–23	4.48E–25	2.13E–24	2.03E–24
287.5	7.30E–24	1.25E–23	4.75E–25	2.40E–24	2.39E–24
288.3	7.00E–24	1.20E–23	4.87E–25	2.52E–24	2.68E–24
289.2	6.62E–24	1.14E–23	5.02E–25	2.67E–24	2.97E–24
290.2	6.25E–24	1.08E–23	5.18E–25	2.84E–24	3.12E–24
290.6	6.11E–24	1.05E–23	5.28E–25	2.94E–24	3.19E–24
291.6	5.80E–24	9.88E–24	5.50E–25	3.18E–24	3.47E–24
292.5	5.53E–24	9.30E–24	5.70E–25	3.40E–24	3.77E–24
293.3	5.29E–24	8.82E–24	5.87E–25	3.58E–24	4.03E–24
294.0	5.06E–24	8.34E–24	6.03E–25	3.76E–24	4.36E–24
294.2	5.00E–24	8.21E–24	6.07E–25	3.81E–24	4.39E–24
294.6	4.87E–24	7.96E–24	6.16E–25	3.90E–24	4.45E–24
295.5	4.60E–24	7.43E–24	6.36E–25	4.12E–24	4.59E–24
296.4	4.32E–24	6.95E–24	6.56E–25	4.34E–25	4.80E–24
297.4	4.01E–24	6.41E–24	6.78E–25	4.58E–25	5.16E–24
298.2	3.76E–24	5.98E–24	6.95E–25	4.77E–25	5.48E–24
299.1	3.49E–24	5.52E–24	7.14E–25	4.97E–25	5.72E–24
269.9	2.65E–26	1.09E–24	9.01E–23	2.16E–23	3.41E–23
270.0	2.74E–26	1.10E–24	9.03E–23	2.15E–23	3.40E–23
270.3	3.29E–26	1.12E–24	9.15E–23	2.12E–23	3.38E–23
270.9	4.38E–26	1.17E–24	9.38E–23	2.05E–23	3.35E–23
271.3	5.25E–26	1.20E–24	9.52E–23	2.02E–23	3.33E–23
271.6	6.21E–26	1.22E–24	9.66E–23	1.98E–23	3.30E–23
271.8	6.75E–26	1.24E–24	9.74E–23	1.96E–23	3.29E–23
272.6	9.49E–26	1.30E–24	1.01E–22	1.87E–23	3.24E–23
273.1	1.13E–25	1.34E–24	1.03E–22	1.82E–23	3.21E–23
274.1	1.51E–25	1.42E–24	1.06E–22	1.71E–23	3.15E–23
274.7	1.84E–25	1.47E–24	1.09E–22	1.64E–23	3.12E–23
275.2	2.15E–25	1.51E–24	1.11E–22	1.59E–23	3.09E–23
275.9	2.63E–25	1.56E–24	1.14E–22	1.54E–23	3.07E–23
276.7	3.21E–25	1.62E–24	1.17E–22	1.47E–23	3.03E–23
277.7	3.98E–25	1.70E–24	1.22E–22	1.38E–23	2.99E–23
278.3	4.58E–25	1.75E–24	1.25E–22	1.33E–23	2.97E–23
278.9	5.28E–25	1.79E–24	1.27E–22	1.29E–23	2.95E–23
279.5	6.02E–25	1.84E–24	1.30E–22	1.23E–23	2.92E–23

Wavelength, nm	C_2H_4O	C_3H_6O	ClONO	$ClONO_2$	$BrONO_2$
280.0	6.57E–25	1.88E–24	1.32E–22	1.19E–23	2.90E–23
281.0	8.21E–25	1.96E–24	1.34E–22	1.13E–23	2.86E–23
281.8	9.82E–25	2.02E–24	1.36E–22	1.08E–23	2.83E–23
282.6	1.18E–24	2.09E–24	1.38E–22	1.03E–23	2.80E–23
283.4	1.39E–24	2.15E–24	1.40E–22	9.79E–24	2.76E–23
283.6	1.45E–24	2.17E–24	1.41E–22	9.67E–24	2.76E–23
284.6	1.74E–24	2.24E–24	1.43E–22	9.05E–24	2.72E–23
285.8	2.10E–24	2.34E–24	1.44E–22	8.41E–24	2.65E–23
287.5	2.60E–24	2.47E–24	1.44E–22	7.58E–24	2.55E–23
288.3	2.43E–24	2.53E–24	1.44E–22	7.21E–24	2.51E–23
289.2	2.34E–24	2.61E–24	1.44E–22	6.75E–24	2.45E–23
290.2	2.47E–24	2.64E–24	1.44E–22	6.31E–24	2.39E–23
290.6	2.51E–24	2.65E–24	1.44E–22	6.14E–24	2.38E–23
291.6	2.61E–24	2.69E–24	1.43E–22	5.78E–24	2.34E–23
292.5	3.55E–24	2.85E–24	1.43E–22	5.46E–24	2.30E–23
293.3	3.95E–24	2.93E–24	1.43E–22	5.19E–24	2.27E–23
294.0	3.92E–24	2.98E–24	1.42E–22	4.92E–24	2.24E–23
294.2	3.92E–24	2.98E–24	1.42E–22	4.85E–24	2.23E–23
294.6	3.76E–24	2.98E–24	1.42E–22	4.70E–24	2.22E–23
295.5	3.51E–24	2.98E–24	1.41E–22	4.43E–24	2.17E–23
296.4	3.27E–24	2.98E–24	1.38E–22	4.21E–24	2.12E–23
297.4	2.88E–24	2.93E–24	1.36E–22	3.96E–24	2.06E–23
298.2	2.97E–24	3.14E–24	1.34E–22	3.75E–24	2.01E–23
299.1	3.48E–24	3.14E–24	1.31E–22	3.54E–24	1.96E–23
269.9	3.74E–23	1.36E–23	6.22E–24	4.50E–22	1.59E–24
270.0	3.73E–23	1.36E–23	6.20E–24	4.50E–22	1.58E–24
270.3	3.68E–23	1.35E–23	6.16E–24	4.51E–22	1.55E–24
270.9	3.59E–23	1.33E–23	6.07E–24	4.52E–22	1.49E–24
271.3	3.53E–23	1.32E–23	6.03E–24	4.53E–22	1.45E–24
271.6	3.48E–23	1.30E–23	5.98E–24	4.53E–22	1.41E–24
271.8	3.45E–23	1.30E–23	5.95E–24	4.54E–22	1.39E–24
272.6	3.32E–23	1.27E–23	5.84E–24	4.55E–22	1.31E–24
273.1	3.24E–23	1.25E–23	5.77E–24	4.56E–22	1.26E–24
274.1	3.08E–23	1.21E–23	5.63E–24	4.58E–22	1.15E–24
274.7	2.99E–23	1.19E–23	5.54E–24	4.59E–22	1.09E–24
275.2	2.91E–23	1.17E–23	5.47E–24	4.60E–22	1.04E–24
275.9	2.83E–23	1.15E–23	5.38E–24	4.60E–22	9.70E–25
276.7	2.73E–23	1.13E–23	5.27E–24	4.60E–22	8.85E–25
277.7	2.60E–23	1.10E–23	5.12E–24	4.60E–22	7.74E–25
278.3	2.52E–23	1.08E–23	5.04E–24	4.60E–22	7.10E–25
278.9	2.45E–23	1.06E–23	4.96E–24	4.60E–22	6.52E–25
279.5	2.37E–23	1.05E–23	4.87E–24	4.60E–22	5.83E–25
280.0	2.31E–23	1.03E–23	4.80E–24	4.60E–22	5.30E–25
281.0	2.26E–23	1.03E–23	4.84E–24	4.56E–22	4.84E–25
281.8	2.21E–23	1.02E–23	4.87E–24	4.53E–22	4.47E–25
282.6	2.17E–23	1.02E–23	4.90E–24	4.50E–22	4.10E–25
283.4	2.13E–23	1.02E–23	4.94E–24	4.46E–22	3.74E–25
283.6	2.12E–23	1.02E–23	4.94E–24	4.46E–22	3.64E–25
284.6	2.06E–23	1.01E–23	4.98E–24	4.42E–22	3.18E–25
285.8	2.00E–23	1.01E–23	5.05E–24	4.38E–22	2.71E–25
287.5	1.93E–23	1.00E–23	5.15E–24	4.35E–22	2.10E–25
288.3	1.89E–23	9.96E–24	5.20E–24	4.34E–22	1.83E–25

TABLE I (continued).

Wavelength, nm	$ClNO_2$	ClNO	HOCl	ClO_3	$COCl_2$
289.2	1.85E–23	9.92E–24	5.25E–24	4.32E–22	1.49E–25
290.2	1.81E–23	9.88E–24	5.31E–24	4.29E–22	1.18E–25
290.6	1.79E–23	9.87E–24	5.35E–24	4.28E–22	1.12E–25
291.6	1.77E–23	9.83E–24	5.43E–24	4.24E–22	9.76E–26
292.5	1.74E–23	9.79E–24	5.50E–24	4.20E–22	8.50E–26
293.3	1.72E–23	9.76E–24	5.56E–24	4.17E–22	7.45E–26
294.0	1.70E–23	9.73E–24	5.62E–24	4.14E–22	6.40E–26
294.2	1.69E–23	9.72E–24	5.64E–24	4.13E–22	6.12E–26
294.6	1.68E–23	9.71E–24	5.67E–24	4.12E–22	5.56E–26
295.5	1.66E–23	9.67E–24	5.74E–24	4.08E–22	4.30E–26
296.4	1.63E–23	9.63E–24	5.81E–24	4.07E–22	4.44E–26
297.4	1.61E–23	9.59E–24	5.89E–24	4.05E–22	4.04E–26
298.2	1.59E–23	9.56E–24	5.96E–24	4.04E–22	3.72E–26
299.1	1.56E–23	9.53E–24	6.02E–24	4.02E–22	3.38E–26
269.9	3.73E–26	4.25E–24	3.03E–26	5.13E–22	5.60E–22
270.0	3.70E–26	4.21E–24	3.00E–26	5.11E–22	5.60E–22
270.3	3.60E–26	4.08E–24	2.94E–26	5.01E–22	5.56E–22
270.9	3.41E–26	3.81E–24	2.82E–26	4.80E–22	5.47E–22
271.3	3.30E–26	3.65E–24	2.75E–26	4.68E–22	5.41E–22
271.6	3.19E–26	3.49E–24	2.68E–26	4.56E–22	5.36E–22
271.8	3.12E–26	3.40E–24	2.64E–26	4.49E–22	5.33E–22
272.6	2.87E–26	3.05E–24	2.48E–26	4.22E–22	5.21E–22
273.1	2.71E–26	2.82E–24	2.38E–26	4.05E–22	5.14E–22
274.1	2.39E–26	2.37E–24	2.18E–26	3.71E–22	4.99E–22
274.7	2.20E–26	2.10E–24	2.06E–26	3.50E–22	4.90E–22
275.2	2.08E–26	1.93E–24	1.96E–26	3.36E–22	4.80E–22
275.9	2.00E–26	1.79E–24	1.83E–26	3.21E–22	4.66E–22
276.7	1.90E–26	1.62E–24	1.67E–26	3.03E–22	4.47E–22
277.7	1.78E–26	1.40E–24	1.46E–26	2.80E–22	4.23E–22
278.3	1.70E–26	1.28E–24	1.34E–26	2.66E–22	4.10E–22
278.9	1.64E–26	1.16E–24	1.23E–26	2.54E–22	3.97E–22
279.5	1.56E–26	1.03E–24	1.10E–26	2.39E–22	3.82E–22
280.0	1.50E–26	9.22E–25	1.00E–26	2.28E–22	3.71E–22
281.0	1.40E–26	8.50E–25	9.50E–27	2.12E–22	3.52E–22
281.8	1.32E–26	7.93E–25	9.10E–27	2.00E–22	3.36E–22
282.6	1.24E–26	7.36E–25	8.70E–27	1.87E–22	3.21E–22
283.4	1.16E–26	6.79E–25	8.30E–27	1.75E–22	3.05E–22
283.6	1.14E–26	6.64E–25	8.20E–27	1.72E–22	3.01E–22
284.6	1.04E–26	5.93E–25	7.70E–27	1.56E–22	2.82E–22
285.8	9.52E–27	5.07E–25	7.10E–27	1.42E–22	2.61E–22
287.5	8.50E–27	3.86E–25	6.25E–27	1.25E–22	2.32E–22
288.3	8.05E–27	3.32E–25	5.88E–27	1.18E–22	2.19E–22
289.2	7.48E–27	2.64E–25	5.40E–27	1.08E–22	2.03E–22
290.2	6.94E–27	2.05E–25	4.94E–27	9.88E–23	1.88E–22
290.6	6.76E–27	2.00E–25	4.76E–27	9.52E–23	1.83E–22
291.6	6.36E–27	1.89E–25	4.36E–27	8.72E–23	1.71E–22
292.5	6.00E–27	1.79E–25	4.00E–27	8.00E–23	1.60E–22
293.3	5.70E–27	1.70E–25	3.70E–27	7.40E–23	1.51E–22
294.0	5.40E–27	1.61E–25	3.40E–27	6.80E–23	1.42E–22
294.2	5.32E–27	1.59E–25	3.32E–27	6.64E–23	1.40E–22
294.6	5.16E–27	1.55E–25	3.16E–27	6.32E–23	1.35E–22
295.5	4.80E–27	1.44E–25	2.80E–27	5.60E–23	1.24E–22
296.4	4.44E–27	1.36E–25	2.72E–27	5.16E–23	1.16E–22
297.4	4.04E–27	1.26E–25	2.52E–27	4.56E–23	1.06E–22
298.2	3.72E–27	1.18E–25	2.36E–27	4.08E–23	9.80E–23
299.1	3.38E–27	1.09E–25	2.19E–27	3.56E–23	8.94E–23

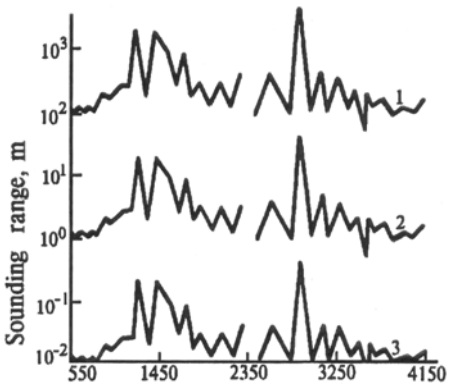

FIG. 2. The maximum admissible (1% error) sounding ranges due to SO_2 *absorption as functions of the Raman shift for the following three media: urban atmosphere (1), stack plume (2), and plant stack input (3).*

CONCLUSIONS

Regardless of a long history of lidar development and many demonstrations of lidar capabilities, not so many lidars are in a routine use. Mostly this is caused by the fact that lidars are primarily aimed at using in a scientific research. However, now when numerous theoretical and experimental investigations have been carried out, the time is right for commercial production of lidars. For solving the ecological problems, in our opinion, a mobile gas and aerosol lidar intended for integrated sounding of stack plumes can be one of them.

All necessary grounds for constructing such a lidar exist, as is shown above. Only a detailed analysis is needed for solving the instrumentation problems and developing the effective algorithms of signal processing based on the above–proposed method.

REFERENCES

1. M.E. Berlyand, *Modern Problems of Atmospheric Diffusion and Atmospheric Pollution* (Gidrometeizdat, Leningrad, 1975).
2. G.E. Landsberg, *Urban Climate* (Gidrometeoizdat, Leningrad, 1983), 448 pp.
3. E.D. Hinkley, ed., *Laser Monitoring of the Atmosphere* (Springer Verlag, Berlin–New York–Heidelberg, 1976), 248 pp.
4. R. Measures, *Laser Remote Sensing* (J. Wiley and Sons, New York, 1974).
5. V.E. Zuev, I.V. Samokhvalov, B.V. Kaul', et al., *Laser Remote Sensing of Industrial Aerosol* (Nauka, Novosibirsk, 1986), 150 pp.
6. V.M. Zakharov and O.K. Kostko, *Meteorological Laser Sensing* (Gidrometeoizdat, Leningrad, 1977), 222 pp.
7. O.K. Kostko, V.S. Portasov, V.U. Khattatov, and E.A. Chayanova, *Laser Applications to the Study of the Atmospheric Composition* (Gidrometeoizdat, Leningrad, 1983), 215 pp.
8. I.V. Samokhvalov, Yu.D. Kopytin, I.I. Ippolitov, et al., *Laser Sounding of the Troposphere and the Underlying Surface* (Nauka, Novosibirsk, 1987), 262 pp.
9. A.I. Popov, ed., *Laser Absorption Analysis and its Applications to Geology, Geophysics, and Ecology* (Energoizdat, Moscow, 1982), 60 pp.

10. I.M. Nazarov, A.N. Nikolaev, and Sh.D. Fridman, *A Foundation of Remote Methods of Monitoring of the Environmental Pollution* (Gidrometeoizdat, Leningrad, 1983), 280 pp.
11. S.I. Dolgii, V.V. Zuev, S.V. Smirnov, and S.F. Shubin, Opt. Atm. **4**, No. 5, 385–388 (1991).
12. G.N. Glazov, *Statistical Problems of Laser Sounding of the Atmosphere* (Nauka, Novosibirsk, 1987), 312 pp.
13. D. Russo, G. Fridman, and P. Williams, *Raman Scattering Spectroscopy in Gases and Liquids* [Russian translation] (Mir, Moscow, 1982), pp. 247–309.
14. V.N. Zakharov, O.K. Kostko, and S.S. Khmelevtsov, *Lidars and Climate Research* (Gidrometeoizdat, Leningrad, 1990), 320 pp.
15. Yu.G. Vainer, L.P. Malyavkin, I.M. Nazarov, et al., Meteorol. Gidrol., No. 12, 39–47 (1980).
16. S.A. Danichkin, V.M. Dubyagin, T.K. Sklyadneva, in: *Abstracts of Reports at the Eleventh Symposium on Laser and Acoustic Sounding of the Atmosphere,* Tomsk (1992).
17. S.S. Vetokhin, I.P. Gulakov, A.N. Pertsev, et al., *Single–Electron Photodetectors* (Energoizdat, Moscow, 1986), 160 pp.
18. Yu.G. Vainer, S.F. Kol'yanov and K.V. Tanana, in: *Spectroscopy of Raman Scattering* (Institute of Spectroscopy, Russian Academy of Sciences, Moscow, 1978), pp. 68–69.
19. V.E. Zuev, Yu.S. Makushkin, and Yu.N. Ponomarev, *Atmospheric Spectroscopy* (Gidrometeoizdat, Leningrad, 1983), 248 pp.
20. I.L. Karol', V.V. Rozanov, and Yu.M. Timofeev, *Gaseous Impurities in the Atmosphere* (Gidrometeoizdat, Leningrad, 1983), 192 pp.
21. V.M. Dubyagin and N.A. Shefer, in: *Abstracts of Reports at the Eleventh Symposium on Laser and Acoustic Sounding of the Atmosphere,* Tomsk (1992).
22. *Reference Book in Geophysics* (Nauka, Novosibirsk, 1965), 572 pp.
23. D.J. Brasington, Appl. Opt., No. 20, 3774–3779 (1981).
24. B.A. Thompson, P. Harteck, and R.R. Reeves, J. Geophys. Res. **68**, No. 24, 6431–6436 (1963).
25. *The Stratosphere. Present and Future,* NASA Ref. Publ. (1979), 432 pp.
26. D.L. Baulch, J. Phys. Chem. **9**, No. 2, 295–471 (1980).
27. H.S. Johnston and R. Graham, J. Phys. Chem. **77**, No. 1, 62–63 (1973).
28. M.Yu. Kataev, A.A. Mitsel', and E.G. Tinchurina, VINITI, No. 4063–85, Moscow, October, 1985.
29. D.J. Seery and D. Britton, J. Phys. Chem. **68**, No. 8, 2263–2266 (1964).
30. H.S. Johnson and R. Graham, J. Phys. Chem. **52**, No. 8, 1415–1423 (1974).
31. E.L. Aleksandrov, I.L. Karol', L.R. Rakipova, et al., *Atmospheric Ozone and Global Climatic Change* (Gidrometeoizdat, Leningrad, 1982), 168 pp.